Journal of Theoretical and Applied Information Technology
31st July 2022. Vol.100. No 14

ISSN: 1992-8645 www.jatit.org E-ISSN: 1817-3195

COMPARATIVE ANALYSIS OF MAXIMUM POWER POINT TRACKING METHOD USING SLIDING MODE AND P&O CONTROLLERS

SANA MOUSLIM[1], M'HAND OUBELLA[1], MOHAMED AJAAMOUM[1], EL MAHFOUD BOULAOUTAQ[1], MOHAMED BENYDIR[1], KAOUTAR DAHMANE[1]

[1]*Laboratory of engineering sciences and energy management (LASIME), Electrical engineering department, ESTA Ibnzohr University, Agadir, Morocco*

E-mail: [1]sana.mouslim@uiz.ac.ma

ABSTRACT

The power delivered by a solar photovoltaic generator (PVG) strongly depends on the level of irradiance G, temperature T of cells, total or partial shading but also the nature of the fueled load. The P_{PV}-V_{PV} power characteristic of the PVG has a maximum power point (MPP) corresponding to the optimal operating point. Since the position of the MPP depends on the level of irradiance and the temperature of the cells, it is never constant over time. Therefore, a control strategy is requisite to extract maximum power from solar panels under all operating conditions. The objective of this work is to design a MPPT controller based on sliding mode controller (SMC) that is applied to a buck-boost converter in order to achieve an optimal PV module output voltage. The proposed MPPT controller using SMC has been developed so that the operating point converges to the optimum operating point. The validation of the proposed controller is shown by MATLAB/SIMULINK simulation. The results confirm the effectiveness of the sliding mode control MPPT under the parameter variation environments. Moreover, a comparison analysis of the proposed SM controller and classical MPPT algorithm using Perturb-and-Observe method has been designed for the same PV power system in order to evaluate the robustness and stability against parameter uncertainties for the two proposed controllers.

Keywords: *Photovoltaic; Buck-Boost converter; MPPT; P&O; Sliding mode control; MATLAB/Simulink.*

1. INTRODUCTION

DC-DC converters constitute an important class of static converters. They are used to supply a load with an adjustable DC continuous voltage source. These converters are widely used in computers, electronic device... to adapt input voltage of a system with the desired output voltage. In the literature, to analyze the behavior of DC-DC converters the state space average (SSA) model is adopted in order to design the appropriate controller [1].

Several techniques are used to control these converters, like the non-linear sliding mode control (SMC), which has been mainly developed for the control of variable structure systems [2][3], and it has two modes of operation. The first mode is called the approaching mode [4], means that the system state converges to a predefined manifold named sliding function. The second mode is called the sliding mode [5][6], where the system state is confined on the sliding surface and is driven to the origin.

The sliding MPPT controller converter is a power conversion system with a suitable control algorithm for extracting the maximum power that the PVG can provide. Several approach to track the MPP has been discussed in many literatures. Among these algorithms, perturbation methods [7], incremental conductance [8] [9], hill-climbing [10] [11]. All these algorithms share the same concept by perturbing the duty cycle (or PV voltage) and observing the output power, which provides useful data for tuning duty cycle [12]. These tracking methods have been widely reported. The P&O MPPT method tends to oscillate around the MPP, which causes power loss and the system efficiency becomes low. The conventional MPPT methods

such as P&O, IC…. have a slow transient response during rapidly changing environmental conditions.

Therefore, contrary to the classic method used in some literature [ ] to find the slip surface based on the calculation of the slip coefficients, the sliding mode control concept modeled in this study is designed to require the system to operate in the maximum power point, otherwise the choice of the sliding surface is equal to the MPP condition.

The objective of the MPPT controller based on SMC, in order to achieve an optimal PV array output voltage, is that the sliding surface set to be the MPP condition, so that the operating point converges to the optimum operating point. The main advantage of the sliding technique is the simplicity of implementation, robustness, and high performance in different fields.

In this paper, the interest was focused in the use of SMC in the photovoltaic fields by maximizing the power generated from the PV panel. The sliding MPPT controller is designed on the characteristics of PV modules. Which are defined for the slip surface as MPP condition in order to operate the PV system near the MPP.

First, the modelling and the sizing of a buck-boost converter in continuous conduction mode (CCM) is presented. The converter was assumed to operate in environment, submitted to disturbances such as the input voltage variation and load variation, which causes the fluctuation of operating point of DC-DC converter. A converter ensuring the MPPT function must be used to follow these changes.

In the second part, the structural analysis of the concept of approaching mode for the sliding surface is introduced, which is defined by $\frac{dP_{pv}}{dV_{pv}}$ =0, (where Ppv and Vpv are the power delivered by the PV panel and the output voltage of the photovoltaic panel). The expression $\frac{dP_{pv}}{dV_{pv}}$ =0 is the condition of the maximum power point PPM. The main role of this controller is to force the system to work at the MPP.

Additionally, The MPPT based on Perturb and Observe method is adopted to our system to maximize the output power and compared to sliding MPPT controller regarding the convergence toward PPM. The robustness of the two proposed MPPT controllers is investigated in the presence of load variations and environment changes due to meteorological conditions.

The paper is organized as follow: Modeling of the photovoltaic PV module is given in the second section. The third section is dedicated to modelling and the sizing of a buck-boost converter. MPPT tracking controller based on P&O method is presented in the fourth section. The proposed MPPT sliding mode control approach is described in the fifth section. The implementation and simulation results are presented in the sixth section. The final section is dedicated to concluding remarks and discusses avenues for further research.

2. MODELING THE PV MODULE

Solar cell is a diode, or electronic junction PN, of large surface, exposed to light (photons), and generates a potential difference, this physical phenomenon called photovoltaic effect [13]. Various mathematical models are commonly developed to represent the behavior of photovoltaic cell. These mathematical models are generally differentiated by the number of parameters and the mathematical procedures involved in the calculation of the photovoltaic module [14].
The photovoltaic cell model of one diode exposed in figure 1, takes into account not only the voltage losses expressed by the R_s series resistor, but also the current leaks expressed by a parallel resistor R_p [12].

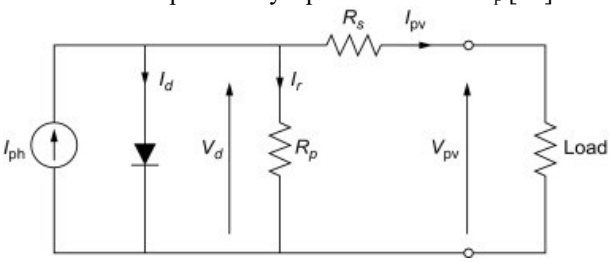

Figure 1: Photovoltaic cell model of one diode

The equivalent circuit can be modeled by the equations below, basing on Kirchhoff 's low [14]:

$$I = I_{ph} - I_d\left(\exp\left(\frac{q}{k_b TA}V\right) - 1\right) \quad (1)$$

$$I_{ph} = S[I_{scr} + k_i(T - T_r)] \quad (2)$$

$$I_d = I_{rr}\left[\frac{T}{T_r}\right]^3 \exp\left(\frac{qE_g}{kQA}\left[\frac{1}{T_r} - \frac{1}{T}\right]\right) \quad (3)$$

I: output current (A).
V: output voltage (V).
T: cell temperature (K).
S: solar irradiance (W/m2).
Iph : light-generated current (A).
Id : PV saturation current (A).
Irr : saturation current at Tr (A).
I_{scr} : short-circuit current at reference condition (A).
T_r : reference temperature (K).

Journal of Theoretical and Applied Information Technology
31st July 2022. Vol.100. No 14

ISSN: 1992-8645 www.jatit.org E-ISSN: 1817-3195

K_i : short-circuit temperature coefficient (A/K).
q : charge of an electron (C).
k_b : Boltzmann's constant ($J.K^{-1}$).
E_g : band-gap energy of the material.
Q: total electron charge (C).
A : ideality factor.

The electrical characteristics of solar PV that used in this work is shown in table 1.

Table 1: Solar panel parameters type PYS240

Parameters	Value
I_{mp}	3.66 A
V_{mp}	17.5 V
$P_{max,e}$	64 W
I_{sc}	4.0144 A
V_{oc}	21.3 V
A	1.2
N_S	36

3. BUCK-BOOST CONVERTER SIZING AND MODELLING

The buck-boost converter is the simplest and most commonly used converter for power regulation. The primary function of the buck-boost converter is that the voltage can be increased or decreased according to the switching mode. However, the output voltage V_{out} have opposite sign to the input voltage V_{in}. There are two operating modes for the buck-boost converter, namely, the CCM and the discontinuous conduction mode [15].

Figure 2 shows the modeling of buck-boost converter on the MATLAB Simulink environment.

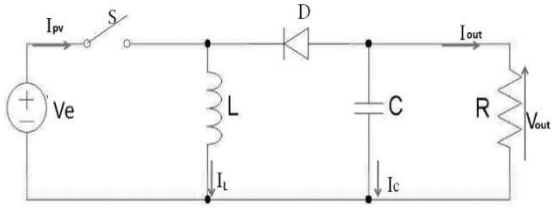

Figure 2: Buck-boost Converter

Our work is based on the modelling and dimensioning of the buck-boost converter in CCM. In this mode, there exist only two switching states in the converter, "S is on and D is off" and "S is off and D is on. In addition, the current crossing the inductor *L* never drops to zero. Therefore, the study is conducted in two operating modes depending on the state of conduction of switch S.

3.1. The Operating Modes of Buck-Boost Converter

Figure 3 shows the ON state of switch *S*: in this case, when the transistor is in the "ON" position, the current in the inductor increases which causes the storage of energy.

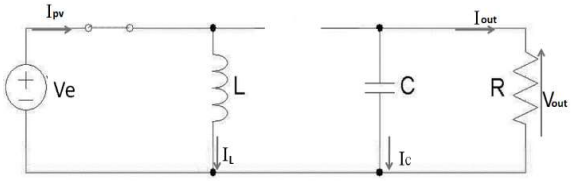

Figure 3: Buck-boost converter when S_1 is closed.

The diode is used to drain the energy stored in the inductance when the switch is blocked. Figure 4 shows the OFF state of the buck-boost converter.

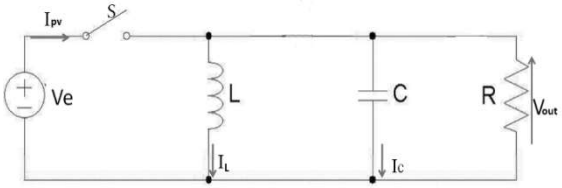

Figure 4: Buck-boost when S_1 is open.

When the switch changes to the "OFF" position, the voltage through the inductance is then reversed and the stored energy is transferred to the load via the diode. In this case, the voltage at the terminals of the load V_{out}, describing the operation in continuous conduction, following the expression bellow [15]:
The duty cycle of the buck-boost converter is:

$$\beta = \frac{V_{out}}{V_{out}+V_{in}} \quad (4)$$

The duty cycle β varies according to the applied input voltage in order to obtain the desired output voltage. For a buck-boost converter, the ripple of the current in the inductance can be demonstrated by [16]:

$$\Delta I_L = \frac{\beta}{L f} \times V_{in} \quad (5)$$

The ripple of the current is influenced by the frequency f of the signal PWM, the duty cycle β and by the L induction coefficient. So, the inductance value is calculated by:

$$L_{min} = \beta \times \frac{1-\beta}{\Delta I_L f} \times V_{in} = \frac{1-\beta}{2 f} \times V_{out} \quad (6)$$

And:

$$C = \frac{V_S \times (1-\beta)}{8 \times L \times f^2 \times \Delta V_{out}} \quad (7)$$

Journal of Theoretical and Applied Information Technology
31st July 2022. Vol.100. No 14

ISSN: 1992-8645 www.jatit.org E-ISSN: 1817-3195

The use of Schottky diodes avoids recovery problems and therefore additional switching losses. The efficient value of the current in the diode will be adopted by:

$$i_{d(eff)} = i_{pv}\sqrt{(1-\beta)}\,\frac{i_{out}}{\sqrt{(1-\beta)}} \quad (8)$$

3.2. Results of Modelling of the Buck-Boost converter

The dimensioning results of the different components of the buck-boost converter are shown in Table 2 bellow:

Table 2: Buck-boost Converter Parameters

Parameters	Value
L	*275 mH*
C	*470 µF*
f	*15 KHz*
R	*100Ω*
β	*50%*
V_{in}	*20 V*
V_{out}	*20 V*

The characteristics of a PV generator depend on methodologic conditions (solar irradiation and temperature), therefore these climatic variations cause the fluctuation of the (MPP).

The buck-boost converter is a vital part of renewable energy conversion. It is essentially used to achieve a regular DC voltage from DC source.it is used in our study as interface between load and PV module, serve the purpose of transferring maximum power from PV module to the load, by changing the duty cycle.

The first part of simulation, consist on applying an adequate control action using the duty cycle. In order to obtain the desired results. Figure 5 shows the open loop of the buck-boost converter with fixed input voltage:

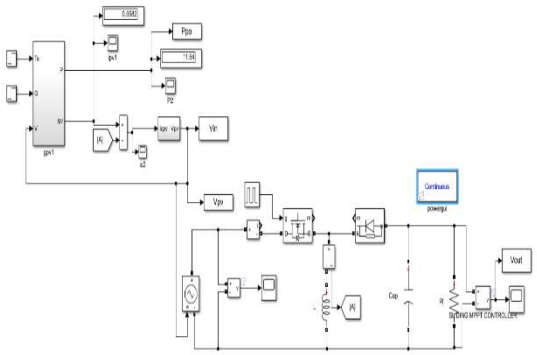

Figure 5: Simulation of the open loop of buck-boost converter

Figure 6 represents the behavior of the output voltage, which converge to 12V after overshoot and oscillation.

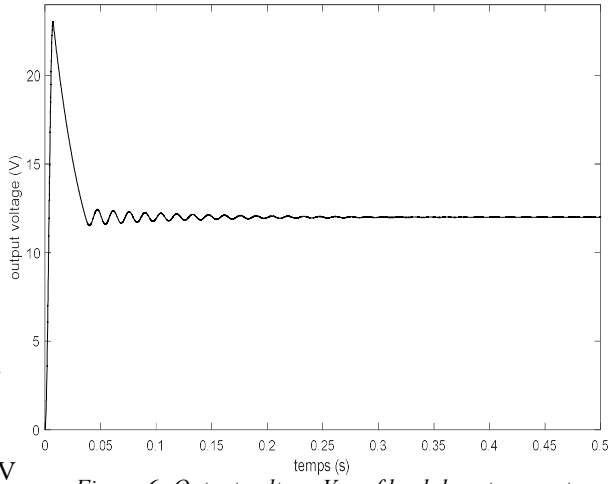

Figure 6: Output voltage V_{out} of buck-boost converter in Open loop

3.3. Modelling of the Buck-Boost converter

A mathematical modelling of DC-DC buck-boost converter is proposed in this section, for different operating states of the switch in CCM. The dynamic equations for the ON state of the mosfet S can be formalizing in the state space as [16]:

$$\dot{X} = AX + Bu \quad (9)$$

$$Y = CX + Du \quad (10)$$

Which implies:

$$\frac{di}{dt} = \frac{V_{in}}{L} \quad (11)$$

$$\frac{dV_c}{dt} = -\frac{V_c}{RC} \quad (12)$$

The representation in state space for the OFF state of the switch S, is transformed into:

$$\frac{di}{dt} = \frac{V_c}{L} \quad (13)$$

$$\frac{dV_c}{dt} = -\frac{i_L}{C} - \frac{V_c}{RC} \quad (14)$$

Using equations (9) to (14) and applying the SSA method translated into equations (15) to (17), the state matrix is obtained as follow:

$$A=A_1\,\beta+A_2(1-\beta) \quad (15)$$

$$B=B_1\,\beta+B_2(1-\beta) \quad (16)$$

$$C=C_1\beta+C_2(1-\beta) \quad (17)$$

$$\begin{bmatrix}\dot{x}_1\\ \dot{x}_2\end{bmatrix} = \begin{bmatrix}0 & \frac{1-\beta}{L}\\ \frac{1-\beta}{C} & \frac{-1}{RC}\end{bmatrix}\begin{bmatrix}x_1\\ x_2\end{bmatrix} + \begin{bmatrix}\frac{\beta}{L}\\ 0\end{bmatrix} V_{in} \quad (18)$$

4. MPPT TRACKING CONTROLLER BASED ON P&O METHOD

The algorithm of MPPT tracking controller based on P&O method works by a disturbance of the system, which mean by increasing or decreasing the operating voltage of the photovoltaic module and observing its effect on the output power [17]. The principle of this controller method is to calculate the voltage and the current V_{pv} and I_{pv}, in order to find the current output power P_{pv} (k) of the PV module. This value P_{pv} (k) is compared to the value P_{pv} (k-1) of the last measurement. If the output power has increased, the disturbance will continue in the same direction. If the power has decreased since the last measurement, the disturbance of the output voltage will be reversed in the opposite direction of the last cycle. When the MPP is reached, V_{pv} will oscillate around the ideal operating voltage. The algorithm shown in Figure 7 illustrates the P&O method [17].

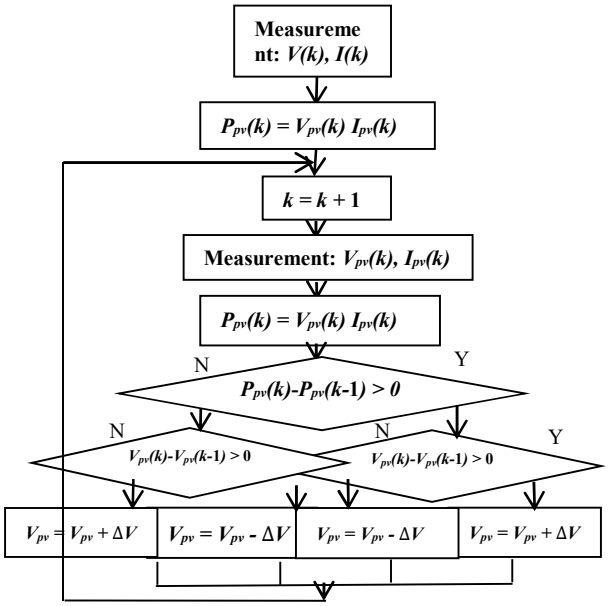

Figure 7: MPPT Tracking Controller based on P&O method

5. SYNTHESIS OF CONTROL LAWS BY SMC FOR BUCK-BOOST CONVERTER

Sliding Mode Control (SMC) is a non-linear type of control, which was originally introduced for the control of variable structural systems. Its main advantages are the guarantee of stability and robustness for wide variations in system parameters, input and disruptions on the system. The technique consists of two modes. One is the approaching mode in which the trajectory moves towards the sliding line from any initial point.

The other is the sliding mode in which, the state trajectory moves to origin along the switching line and the states never leave the switching line. In this study, we introduce the concept of the approaching mode.

The synthesis of a SMC can be summarized into several steps: The choice of the sliding surface, checking the attractiveness of the sliding surface, the demonstration of the existence of the sliding mode and the study of the stability of the control on the sliding surface.

The first step in the design of the control is the choice of the switching surface, which can be selected as follows:

$$\frac{dP_{pv}}{dI_{pv}} = \frac{dI_{pv}^2\,R_{pv}}{I_{pv}} = I_{pv}\left(2R_{pv} + I_{pv}\frac{dR_{pv}}{dI_{pv}}\right) = 0 \quad (19)$$

Knowing that the condition of the maximum power point PPM is given by:

$$\frac{dP_{pv}}{dV_{pv}} = 0 \quad (20)$$

where $R_{PV} = V_{pv}/I_{pv}$ is the equivalent load connect to the PV, and I_{PV} is the PV current, which is equal to i_L .The non-trivial solution of the equation (19) is $2R_{pv} + I_{pv}\frac{dR_{pv}}{dI_{pv}}$. Hence, the sliding surface is defined as:

$$\gamma = 2R_{pv} + I_{pv}\frac{dR_{pv}}{dI_{pv}} \quad (21)$$

If we take the P-V characteristics of the PVG for given meteorological conditions. Depending on the slope of the curve, we can divide the figure into two zones separated by the point PPM (γ=0). Zone 1 for which the slope is positive γ < 0, and zone 2 for which the slope is negative γ > 0. If, for example, the working point is to the left of the MPP, the control must move towards the sliding surface by increasing the voltage V_{pv} and if, on the contrary, the working point is located to the right of the PPM, the control must move it towards the sliding surface by decreasing the voltage V_{pv}.

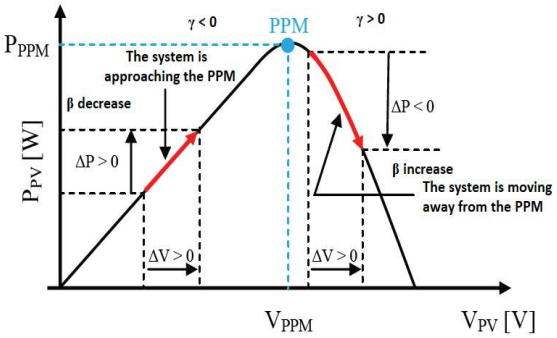

Figure 8: The characteristics P-V of the solar panel

For this, the switching control law adopted is that presented by the equation:

$$u = \begin{cases} \beta + \Delta\beta & \text{for} \quad \gamma > 0 \\ \beta - \Delta\beta & \text{for} \quad \gamma < 0 \end{cases} \quad (22)$$

Consider a nonlinear time-dependent switching system defined by the following equation [13]:

$$\dot{x}(t) = g(x(t)) + \phi(x(t)).u(t) \quad (23)$$

where x(t) is the state-variable vector in an n-dimensional space R^n; g(.) and ϕ(.) are smooth vector fields in the same space; and u(t) is the discontinuous control action. The replacement of the discontinuous control action u(t) by a continuous control action $u_{eq}(t)$ into (23) converts the switching SM system into an average continuous SM system given as:

$$\dot{x}(t) = g(x(t)) + \phi(x(t)).u_{eq}(t) \quad (24)$$

The equivalent control is determined from the following condition:

$$\dot{\gamma} = [\frac{d\gamma}{dX}]^T\dot{X} = [\frac{d\gamma}{dX}]^T(f(X) + g(X)u_{eq}) = 0 \quad (25)$$

The equivalent control can be obtained by the following expression:

$$u_{eq} = -\frac{\left[\frac{d\gamma}{dX}\right]^T f(X)}{\left[\frac{d\gamma}{dX}\right]^T g(X)} = 1 - \frac{V_{in}}{V_{out}} \quad (26)$$

The positive LYAPUNOV function is defined as $V = \frac{1}{2}\gamma^2$, so that the surface γ=0 is attractive, it is enough that the derivative compared at the time of V either negative (condition called: attractiveness condition or reachability):

$$\dot{V} = \dot{\gamma}\gamma < 0\,, \quad \forall\, \gamma \neq 0 \quad (27)$$

To prove this theorem of the existence of the sliding mode, we calculate the derivative of the surface γ:

$$\dot{\gamma} = [\frac{d\gamma}{dX}]^T\dot{X} = (2R_{pv} + I_{pv}\frac{dR_{pv}}{dI_{pv}})'\left(-\frac{1-\beta}{L}V_{out} + \frac{\beta}{L}V_{in}\right) \quad (28)$$

$$\dot{\gamma} = [\frac{d\gamma}{dX}]^T\dot{X} = \left(3\frac{dR_{pv}}{dI_{pv}} + I_{pv}\frac{d^2R_{pv}}{dI_{pv}^2}\right)\left(-\frac{1-\beta}{L}V_{out} + \frac{\beta}{L}V_{in}\right) \quad (29)$$

Replacing R_{PV} by the definition $R_{PV} = V_{PV}/I_{PV}$ we found:

$$\frac{dR_{pv}}{dI_{pv}} = \frac{d\left[\frac{V_{pv}}{i_{pv}}\right]}{di_{pv}} = \frac{1}{i_{pv}}\frac{dV_{pv}}{di_{pv}} - \frac{V_{pv}}{i_{pv}^2} \quad (30)$$

$$\frac{d^2R_{pv}}{dI_{pv}^2} = \frac{1}{i_{pv}}\frac{d^2V_{pv}}{dI_{pv}^2} - \frac{2}{i_{pv}^2}\frac{dV_{pv}}{di_{pv}} + \frac{2V_{pv}}{i_{pv}^3} \quad (31)$$

The mathematical form of the equivalent model can be given as (1)–(3). Where R_s is relatively small and R_{sh} is relatively large, which are neglected in the equation in order to simplify the simulation. The PV voltage V_{PV} can be rewritten as function of PV current I_{PV} :

$$V_{pv} = \frac{k_bTA}{q}\ln\left(\frac{I_{ph} + I_d - I_{pv}}{I_d}\right) \quad (32)$$

$$\frac{dV_{pv}}{dI_{pv}} = -\frac{k_b TA}{q}\frac{I_0}{I_{ph}+I_0-I_{pv}} < 0 \quad (33)$$

$$\frac{d^2V_{pv}}{dI_{pv}^2} = -\frac{k_b TA}{q}\frac{I_0}{(I_{ph}+I_0-I_{pv})^2} < 0 \quad (34)$$

So, the first term of the surface derivative becomes:

$$\left[\frac{d\gamma}{dX}\right]^T = 3\frac{dR_{pv}}{dI_{pv}} + I_{pv}\frac{d^2R_{pv}}{dI_{pv}^2} = \frac{1}{i_{pv}}\frac{dV_{pv}}{di_{pv}} - \frac{V_{pv}}{i_{pv}^2} + \frac{d^2V_{pv}}{dI_{pv}^2} < 0 \quad (35)$$

Based on the results of equation (33) and (34) and according to the sign of the expression $\frac{V_{pv}}{i_{pv}^2} > 0$, the sign of the equation (35) is clearly negative. The condition of $\gamma = 0$ will be fulfilled if only if $\gamma\dot{\gamma} < 0$ for all β cases discussed as follows:

For $0 < \boldsymbol{\beta} < 1$

$$\dot{X} = -\frac{1-\beta}{L}V_{out} + \frac{\beta}{L}V_{in} \quad (36)$$

$$\dot{X} = -\frac{1-(U_{eq}+K\gamma)}{L}V_{out} + \frac{(U_{eq}+K\gamma)}{L}V_{in} \quad (37)$$

since the range of duty cycle must be between$0 < U_{eq} < 1$, the control signal proposed is:

$$\beta = 1 \quad for \quad u_{eq} + k\gamma \geq 1 \quad (38)$$

$$\beta = u_{eq} + k\gamma \quad for \quad 0 < u_{eq} + k\gamma < 1 \quad (39)$$

$$\beta = 0 \quad for \quad u_{eq} + k\gamma \leq 0 \quad (40)$$

In this case of the duty cycle:

$$\dot{X} = \frac{k\gamma}{L}(V_{out} + V_{pv}) - \frac{V_{pv}^2}{V_{out}} \quad (41)$$

It is necessary to prove that $\dot{\gamma}\gamma < 0$ whatever the sign of the sliding surface γ for $0 < \beta < 1$.
For $\boldsymbol{\gamma} < 0$:

$$\dot{X} = \frac{k\gamma}{L}(V_{out} + V_{pv}) - \frac{V_{pv}^2}{V_{out}} < 0 \quad (42)$$

In addition, we have:

$$\left[\frac{d\gamma}{dX}\right]^T < 0 \quad (43)$$

So:

$$\dot{\gamma} = \left[\frac{d\gamma}{dX}\right]^T \dot{X} > 0 \quad (44)$$

For $\gamma < 0$

The product of the surface and its derivative is negative $\dot{\gamma}\gamma < 0$
For $\boldsymbol{\gamma} > 0$:
To have $\dot{\gamma}\gamma < 0$ it is necessary to prove that $\dot{X} > 0$ for the two possible cases of V_{out} and V_{pv}
For $V_{pv} > V_{out}$:

$$\dot{X} = \frac{k\gamma}{L}\left(1 + \frac{V_{pv}}{V_{out}}\right) - \frac{V_{pv}^2}{V_{out}^2} \quad (45)$$

With:

$$\frac{V_{pv}^2}{V_{out}^2} > 1 \quad \text{and} \quad 1 + \frac{V_{pv}}{V_{out}} > 2 \quad (46)$$

So:

$$\left(1 + \frac{V_{pv}}{V_{out}}\right) - \frac{V_{pv}^2}{V_{out}^2} > 1 \quad (47)$$

Since we have a positive sliding surface therefore:

$$\frac{k\gamma}{L}\left(1 + \frac{V_{pv}}{V_{out}}\right) > \frac{V_{pv}^2}{V_{out}^2} \quad (48)$$

Which implied that the product $\gamma\dot{\gamma}$ is negative for $V_{pv} > V_{out}$.
For $V_{pv} < V_{out}$:

$$\frac{V_{pv}^2}{V_{out}^2} < 1 \quad \text{and} \quad 1 + \frac{V_{pv}}{V_{out}} < 2 \quad (49)$$

So:

$$\frac{k\gamma}{L}\left(1 + \frac{V_{pv}}{V_{out}}\right) - \frac{V_{pv}^2}{V_{out}^2} > 1 \quad (50)$$

The stability condition $\gamma\dot{\gamma} < 0$ is verified for the different cases of the sliding surface γ, the input and output voltage.
For $\boldsymbol{\beta} = 1$

$$\dot{X} = \frac{1}{L}V_{in} > 0 \quad (51)$$

By the equation (35) and (51), the sign of $\dot{\gamma}$ is negative.
With $\boldsymbol{\beta} = 1$ two cases should be discussed for the accomplishment of $\gamma\dot{\gamma} < 0$:

- The first case when $u_{eq} = 1$ which implies that the input voltage is equal to 0, and the system works in the left part of the figure, which means that the sliding surface is

Journal of Theoretical and Applied Information Technology
31st July 2022. Vol.100. No 14

ISSN: 1992-8645 www.jatit.org E-ISSN: 1817-3195

negative. Therefore $u_{eq} + k\gamma$ must be less than 1.

- The second case when $u_{eq} < 1$ and $u_{eq} + k\gamma \geq 1$ it implies that the surface is positive $\gamma > 0$ so $\gamma\dot{\gamma} < 0$.

For $\boldsymbol{\beta} = 1$ the stability condition is verified $\gamma\dot{\gamma} < 0$.

For $\boldsymbol{\beta} = 0$ we have $\dot{X} = -\frac{1}{L}V_{out}$ it results that $\dot{\gamma} > 0$, two cases should be discussed as follow:

- The first case when $u_{eq} = 0$ which implies that the input voltage equal to the output voltage. and based on the figure 8 the system is operating in the region $\gamma > 0$.
- The second case when $u_{eq} > 0$ and $u_{eq} + k\gamma \leq 0$ which means that $\gamma < 0$ and $\dot{\gamma}\gamma < 0$.

For $\boldsymbol{\beta} = 0$ the stability condition is verified $\gamma\dot{\gamma} < 0$.

6. SIMULATION AND RESULTS

This section presents the simulation results of the MPPT method based on SMC. In order to test the robustness and speed of the controller, the simulation consists in varying the input voltage by changing the environment conditions of the PV panel and by changing different value of the load during a period of 1s. The results obtained are presented in figure 9 to figure 12. The proposed MPPT is evaluated from two aspects: robustness to variable input voltage (due to meteorological conditions) and variable load, in order to evaluate the efficiency of the controller against parameters uncertainties.

In figure 9, sliding MPPT controller is tested under fixed input voltage of 12V and variable load from 80Ωto 100Ω. As shown in figure bellow, the SMC is able to maintain the output voltage at optimum point and it is robust to the uncertainties parameters (variation of the external conditions).

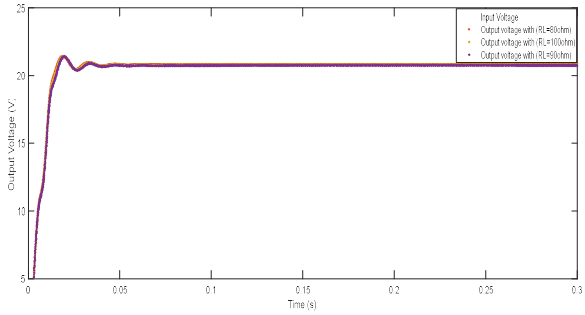

Figure 9: Simulation of the output voltage V_{out} with (V_{in} =21V for (T=25˚C and G =800 W/m²), R_L=100Ω, R_L= 90 Ω and R_L=80 Ω)

Figure 10 and figure 11 represent the response and the behavior of the buck-boost converter for the proposed input voltage changes and load change with MPPT method based on SMC controller.

From the interpretation of the two figures we can clearly conclude that the proposed MPPT controller follow the reference voltage regardless the input voltage variation and load variation. The proposed MPPT controller system attempts to correct the input voltage variation by changing automatically the duty cycle, and by following the desired output voltage. The main advantage of MPPT system with SMC as shown in figure 10 and figure 11 is that it has guaranteed stability and robustness against external variations

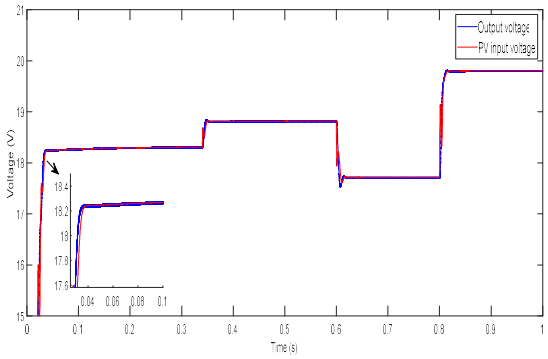

Figure 10: Simulation of the output voltage V_{out} with (T=25˚C → 40˚C, R_L=100Ω)

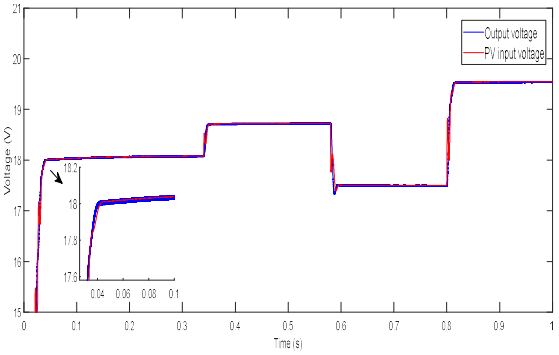

Figure 11: Simulation of output voltage V_{out} with (T=25˚C → 40˚C, R_L=80Ω)

In order to evaluate the robustness and the efficiency of each MPPT controller method, concerning the convergence toward the MPP, figure 12 represent the behavior of the two MPPT controller (P&O method and SMC) for different input voltage changing. we compare through simulations, the convergence towards the MPP

concerning the output voltage of the PV module by using the two MPPT proposed controllers P&O and SMC:

- The settling time of the MPPT controller based on SMC method is around 12ms which is faster than the one of the MPPT based on P&O that is around 28ms.
- The MPPT based on P&O method shows lot of oscillations around the MPP, which causes power loss whereas the SMC remain quite stable.
- The main advantage of the MPPT controller based on SM as shown in figure 12 is the stability and robustness against the input variation and load variation.

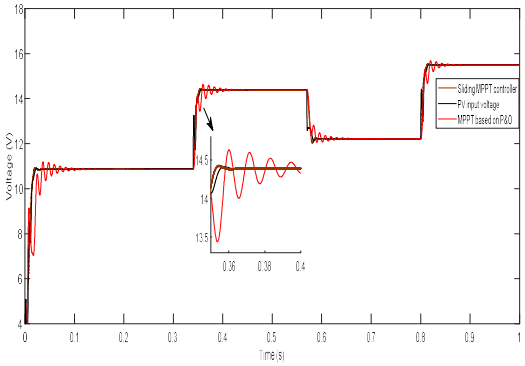

Figure 12: Comparison Of Convergence Towards The PPM Using MPPT Based On P&O Method And Sliding MPPT Controller With Variable Input

In order to check the quality of each model, statistical analysis is performed using the mean absolute percentage error (MAPE).it is a static assessment tool that helps in terms of percentage to measure the size of the error. In order to calculate this index, we start by calculating the relative error, which is equal the absolute error between the simulated and real voltage, divided by the absolute value of the actual voltage as shown in the equation (52) and (53):

$$e = \frac{V_A - V_F}{V_A} \quad (52)$$

$$MAPE = \left(\frac{1}{N}\sum_{i=1}^{N}|e_i|\right) \times 100 \quad (53)$$

where V_A is the actual value and V_F is the forecast value.

Table 3 show the results of the mean absolute percentage error for the two MPPT controllers.

Table 3: Mean Absolute Percentage Error For The Two MPPT Controllers

Controller	Sliding MPPT	P&O algorithm
MAPE	3,9124%	10.6541%

The results of the statistical analysis confirmed that sliding MPPT controller is better performed than the P&O algorithm controller (MAPE = 10.6541% for the P&O algorithm and MAPE= 3,9124 % for the sliding MPPT controller).

In order to measure the efficiency of each MPPT controller, the percentage of power losses of the controller system is calculated compared to the maximum power that a PV system could produce.

This efficiency η_{MPPT} is defined as follows:

$$\eta_{MPPT} = \frac{\int_0^t P_m(t)\,dt}{\int_0^t P_{max}(t)\,dt} \quad (54)$$

Table 4 show the efficiency of the two MPPT controllers.

Table 4: The Efficiency Of The Two MPPT controllers.

Controller	Sliding MPPT	P&O algorithm
η_{MPPT}	99.21%	94.63%

In order to improve the performance criteria of the two MPPT controllers, the hybrid technique is proposed as a prospect that includes the P&O based sliding mode MPPT controller, using an improved fast slip surface. In addition, the proposed controller is implemented in a PV system, so that the control system can track all operating points in normal situations and uncertain conditions. The experimental application of this comparative study designed to maximize the output power of the static DC-DC converter is also proposed as a perspective for this work in order to validate and enhance the statistical analysis of the two controllers

7. CONCLUSION

An ideal SM control operates theoretically at an infinite switching frequency so that the trajectory follows exactly the reference track. This requirement for operating at infinite switching frequency may result in switching losses and may be a source of noise in the system. Hence, for SM control to be applicable to practical systems, the switching frequency of the control implementation must be confined within a practical range. The conventional sliding mode has a defect named the chattering

phenomenon. Plenty of research papers focuses on elimination chattering by using different methods. Including this methods the design of high order sliding mode control, which can eliminate chattering fundamentally

This paper presents the sizing and the modelling of a buck-boost converter in continuous conduction mode. The state space average model was settled and simulated in MATLAB/Simulink environment. The converter was operating in disturbances environment including the input voltage changing (due to meteorological conditions) and load variation.

The MPPT based on the SMC is applied to the PV model and compared to the MPPT based on P&O method. The results show that the dynamic behavior of the two systems is very much different. The MPPT controller with SM method is more efficient based on the response time, which is around 12 ms, against 28 ms for MPPT based on P&O method. however, the modeling of our system with P&O MPPT controller method leads to overshoot with every input voltage changing and oscillations around the reference point. While the MPPT SMC controller has less oscillations once the reference point is reached, which make the system stable and robust against parameter uncertainties. Moreover, to check and measure the size of the error of each model, statistical analysis is performed using the mean absolute percentage error (MAPE) which confirmed that sliding MPPT controller is more performed than the MPPT controller based on P&O algorithm (MAPE = 3,9124% for the SMC and MAPE= 10.6541% for the P&O algorithm).

REFERENCES

[1]. Antip Ghosh and Mayank Kandpal. 2010.State-space average Modeling of DC-DC Converters with parasitic in Discontinuous Conduction Mode (DCM). Department of Electrical Engineering National Institute of Technology, Rourkela

[2]. Tan, Siew-Chong, Yuk-Ming Lai, et Chi Tse. 2012. Sliding Mode Control of Switching Power Converters: Techniques and Implementation. Sliding Mode Control of Switching Power Converters: Techniques and Implementation. https://doi.org/10.1201/9781315217796.

[3]. H. Gohar Ali, R. Vilanova Arbos, J. Herrera, A. Tobón, et J. Peláez-Restrepo, « Non-Linear Sliding Mode Controller for Photovoltaic Panels with Maximum Power Point Tracking », *Processes*, vol. 8, nº 1, p. 108, janv. 2020, doi: 10.3390/pr8010108.

[4]. A. Shahdadi, S. M. Barakati, et A. Khajeh, « Design and implementation of an improved sliding mode controller for maximum power point tracking in a SEPIC based on PV system », *Eng. Rep.*, vol. 1, nº 4, nov. 2019, doi: 10.1002/eng2.12042.

[5]. M. Farhat, O. Barambones, et J. A. Ramos, « MAXIMUM POWER POINT TRACKING CONTROLLER BASED ON SLIDING MODE APPROACH », p. 7, 2014.

[6]. J. S. *et al.*, « Comparative Study of the Performance of Three Modeling Approaches for a Photovoltaic Panel Emulator based on the Single diode Model and Using a Buck-boost DC/DC Converter », *Int. J. Psychosoc. Rehabil.*, vol. 24, nº 03, p. 633-644, févr. 2020, doi: 10.37200/IJPR/V24I3/PR200820.

[7]. Femia, N., G. Petrone, G. Spagnuolo, et M. Vitelli. 2005. « Optimization of perturb and observe maximum power point tracking method ». *IEEE Transactions on Power Electronics* 20 (4): 963-73. https://doi.org/10.1109/TPEL.2005.850975

[8]. Abderrahim, Taouni, Touati Abdelwahed, et Majdoul Radouane. 2020. « Improved Strategy of an MPPT Based on the Sliding Mode Control for a PV System ». *International Journal of Electrical and Computer Engineering (IJECE)* 10 (3): 3074. https://doi.org/10.11591/ijece.v10i3.pp3074-3085.

[9]. Koutroulis, E., K. Kalaitzakis, et N.C. Voulgaris. 2001. « Development of a microcontroller-based, photovoltaic maximum power point tracking control system ». *IEEE Transactions on Power Electronics* 16 (1): 46-54. https://doi.org/10.1109/63.903988.

[10].Xiao, Weidong, et W.G. Dunford. 2004. « A modified adaptive hill climbing MPPT method for photovoltaic power systems » .In,3:1957-1963Vol.3. https://doi.org/10.1109/PESC.2004.1355417.

[11]. Ahmad, Fahad Faraz, Chaouki Ghenai, Abdul Kadir Hamid, et Maamar Bettayeb. 2020. « Application of Sliding Mode Control for Maximum Power Point Tracking of Solar Photovoltaic Systems: A Comprehensive Review ». Annual Reviews in Control 49 (janvier): 173-96. https://doi.org/10.1016/j.arcontrol.2020.04.011.

[12].Chu, Chen-Chi, et Chieh-Li Chen. 2009. « Robust Maximum Power Point Tracking

Method for Photovoltaic Cells: A Sliding Mode Control Approach ». Solar Energy 83 (8): 1370-78. https://doi.org/10.1016/j.solener.2009.03.005.

[13]. « A new maximum power point method based on a sliding mode approach for solar energy harvesting - Science Direct ».s. d. Consulté le 8 octobre 2021. https://www.sciencedirect.com/science/article/abs/pii/S0306261916303750.

[14]. Jenkal, Samia, Mustapha Kourchi, Driss Yousfi, Ahmed Benlarabi, Mohamed Larbi Elhafyani, Mohamed Ajaamoum, et Mhand Oubella. 2020. « Development of a Photovoltaic Characteristics Generator Based on Mathematical Models for Four PV Panel Technologies ». International Journal of Electrical and Computer Engineering (IJECE) 10 (6): 6101. https://doi.org/10.11591/ijece.v10i6.pp6101-6110.

[15].Ghazanfari, J, et M Maghfoori Farsangi. 2013. « Maximum Power Point Tracking Using Sliding Mode Control for Photovoltaic Array ». Electronic Engineering 9 (3): 8.

[16].Gupta, Ankit, Yogesh K. Chauhan, et Rupendra Kumar Pachauri. 2016. « A Comparative Investigation of Maximum Power Point Tracking Methods for Solar PV System ». Solar Energy 136 (octobre): 236-53. https://doi.org/10.1016/j.solener.2016.07.001.

[17].Lyden, S., et M. E. Haque. 2015. « Maximum Power Point Tracking Techniques for Photovoltaic Systems: A Comprehensive Review and Comparative Analysis ». Renewable and Sustainable Energy Reviews 52 (décembre): 1504-18. https://doi.org/10.1016/j.rser.2015.07.172.